Frequency spectrum characterization of terahertz emission from laser-induced air plasma

Ji Zhao (赵 骥)[1], Liangliang Zhang (张亮亮)[2], Yiman Luo (骆怡蔓)[2], Tong Wu (吴 同)[2], Cunlin Zhang (张存林)[2], and Yuejin Zhao (赵跃进)[1*]

[1]*Beijing Key Laboratory for Precision Optoelectronic Measurement Instrument and Technology, School of Optoelectronics, Beijing Institute of Technology, Beijing 100081, China*

[2]*Beijing Key Laboratory for Terahertz Spectroscopy and Imaging, Key Laboratory of Terahertz Optoelectronics, Ministry of Education, Capital Normal University, Beijing 100048, China*

**Corresponding author: yjzhao@bit.edu.com*

Received April 2, 2014; accepted April 29, 2014; posted online July 18, 2014

Terahertz (THz) emission from laser-induced air-plasma is presented. The frequency spectra of THz wave are investigated using an air-biased-coherent-detection method. The frequency spectra are measured under different pump-pulse and probe-pulse energies. The frequency spectra become narrow with the increasing pump power and we speculate it caused by collision behavior. Meanwhile, the bandwidth of the frequency spectra is broadened by the increasing probe power, which can be explained by pulse compression. Based on this finding, the optimal frequency spectrum of THz can be achieved by regulating the probe and pump beam.

OCIS codes: 320.7090, 320.7110, 240, 6380.
doi: 10.3788/COL201412.083201.

The intense terahertz (THz) waves generated from air-induced plasma serve as broadband THz source for sensing and imaging applications. The generation of THz waves from air-induced plasma was first predicted in 1993 and explained by the acceleration of electrons and ions driven by a ponderomotive force[1−7]. Hamster *et al.* experimentally observed this phenomenon. Among the different methods of THz generation and detection, THz gas photonics has attracted the interests of researchers in recent years owing to its broad spectral coverage and scalability. The underlying mechanism was initially understood as a four-wave mixing (FWM) process in ionized air plasma[8,9]. THz time-domain spectroscopy (TDS) uses a laser pulse focused through a type-I beta barium borate (BBO) crystal to generate its second harmonic (SH) along with a THz wave at the ionizing plasma spot[10,11]. However, most researches focus on THz wave energy and signal determinants of the dynamic range, rather than on the spectrum width. The spectrum width can influence the spectral line shapes of absorption and dispersion in biology research as well. So it is the spectrum that matters in the present researches. The THz air-biased-coherent-detection (ABCD) system uses recycled gas as both the production and the detection medium, enabling research on the spectral width of THz waves without the bandwidth limitations such as the electromagnetic echo or phono shocks[12−15]. This system uses a local oscillator to enhance THz wave detection sensitivity by mixing an optical field, a THz field, and a biased electric field (local oscillator) in air. The broadband THz waves generated from laser-induced air plasma can cover the entire THz frequency.

In this letter, we develop an ABCD system to investigate the characterization of the THz frequency spectrum generated in the presence of laser-induced air plasma at different pump and probe power. The variation of the frequency bandwidth of the THz wave generated by air plasma with increasing probe and pump power is observed. Frequency spectrum has been broadened with the increase of probe power, and compressed with the increase of pump power. We speculate the reason of phenomenon by the collision of atomic or molecular and pulse compression. This study reveals that the THz frequency spectrum can be controlled simply by changing the pump and probe power to obtain the desired frequency range.

A schematic diagram of the experimental setup is shown in Fig. 1. The input laser pulse is generated from a regenerative p-polarized Ti:sapphire laser, with repetition rate of 1 kHz, pulse duration of 50 fs, and central wavelength of 800 nm. The laser beam is split into two. The stronger beam, which is called the pump beam, is focused using a lens with focal length of 150 mm to generate THz waves; the other beam, the probe beam, is used to detect THz waves. A 100-μm-thick type-I BBO crystal is used between the lens and the focal spot to generate SH pulse. Both the fundamental and SH pulses mix at the focal point, producing a THz pulse through a process similar to four-wave rectification during the formation of a laser-induced plasma, which produces intense, highly directional, broadband THz emission. The THz wave, after passing through a silicon wafer, which is used to block the residual optical reflection from the lens, is focused, then collimated, and refocused using four parabolic mirrors (PMs) (4-inch focal length). The probe beam is focused using a 125-mm convex lens through a hole in the back of the 4th parabolic mirror (PM4). The THz and optical beams are then focused collinearly to the same spot, where the SH field is induced by THz field. A pair of wire-shaped electrodes with 1-mm gap is placed at the beam focus point, and an AC bias of $\sim$2 kV at 500 Hz (synchronized with the laser repetition rate) is applied to the electrodes. Finally, the SH beam is filtered using a pair of 400-nm bandpass filters and directed into a photomultiplier tube (PMT). The area in

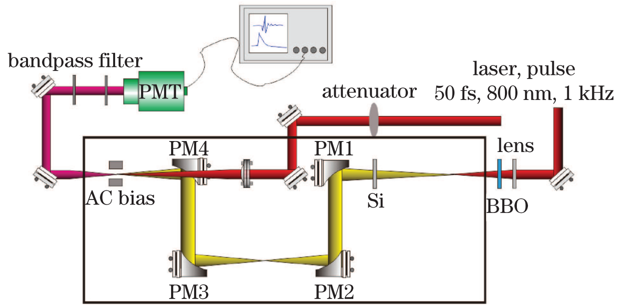

Fig. 1. Experimental setup showing the ABCD THz-TDS system. The PMT is used to detect the second harmonic (2ω), which indirectly shows the THz waves.

the black rectangle is purged by the dry nitrogen gas to eliminate the water absorption lines.

Important information on the collision behavior is obtained through the width of broadened spectral lines from optical to microwave frequencies. We can also find that in low frequencies such as THz, collision would strongly affect the width and shape of a spectral line. In our experiments, we measured the THz power at different pump intensities remaining the probe power unchanged. A fast Fourier transform is performed in the time-domain spectrum. Figure 2 shows the time-domain THz waveform at different pump powers ranging from 400 to 800 mW. As the pump intensity increases from 400 to 800 mW, the bandwidth of the THz spectrum is broadened.

Since the THz spectrum changes as the pump power increases, the bandwidth of THz is calculated under each pump power. We measure the full width at half maximum (FWHM) of the THz frequency spectrum to indicate the bandwidth of the THz. The curve in Fig. 3 shows the trend of FWHM as the pump power increases. It can be seen in Fig. 3 that the width of the frequency spectrum narrows when we increase pump power. The FWHM of THz is 3.72 THz when the pump power is 400 mW. And after increasing the laser power to 800 mW, the FWHM decreases to 2.68 THz. This phenomenon may be attributed to the collision behavior. The electrons and ions collide with each other, then after a collision, the electrons and ions are oriented randomly which can cause the frequency spectrum to change from optical to microwave frequencies[16]. According to motivation theory, with the increasing number of the ions per unit volume, the collision behavior is more intense. THz wave is generated by FWM in the presence of laser-induced air plasma and simultaneously the electrons, ions, and neutral particles which exist in the plasma collide with each other. The interactions of the surrounding electrons, ions, and neutral particles can lead to interference in the plasma state.The width of the frequency is influenced by the molecular dynamics during a collision. Molecules after collision are oriented randomly with respect to the driving field during the collision behavior, leading to the change of some polarization in THz[16]. The optimal THz field achieves maximum when all waves (fundamental wave, SH, and THz waves) are at the same polarization in the FWM process. Nonlinearity appears because of this collision behaviour. Then it can cause the spatial asymmetry of laser induced plasma. As the pump power increases, there will be more free electrons existing and colliding with each other. With the collision becoming more intense, this spatial asymmetry increases obviously which will give rise to intense self-phase modulation of the optical pulse and further cause the narrowing of the THz spectrum width.

In ABCD system, the THz wave propagated collinearly with the probe beam and was focused at the same location. Utilizing the tensor property of third order nonlinear susceptibility, SH pulses with two orthogonal polarizations are detected by two separated PMT simultaneously. So the probe beam also affects the THz frequency spectrum. To further discuss the origin of frequency spectrum changing, we fix the power of the pump laser at 800 mW and change the probe power from 60 to 180 mW. The results are shown in Fig. 4.

THz frequency spectrum broadened in which is different from the way when changing the pump power. With the increase of probe power, the FWHM of the frequency-domain spectrum also increases, as shown in Fig. 5. The collision behavior will not influence the spectrum frequency as the probe beam has no condition of generating plasma. Unlike the case of changing pump power, the broadening of frequency spectrum may be caused by pulse compression which contributes to the self-focusing effect in the air. As the probe power increases, the intensity of the probe beam focused at the electrode is gradually increasing, and the femtosecond laser pulse becomes

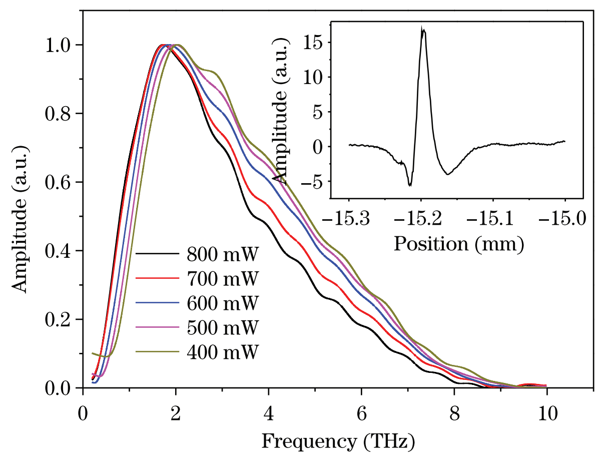

Fig. 2. Normalized amplitude frequency-domain spectrum through fast Fourier transform under different pump powers. Upper right corner: time-domain THz waveform.

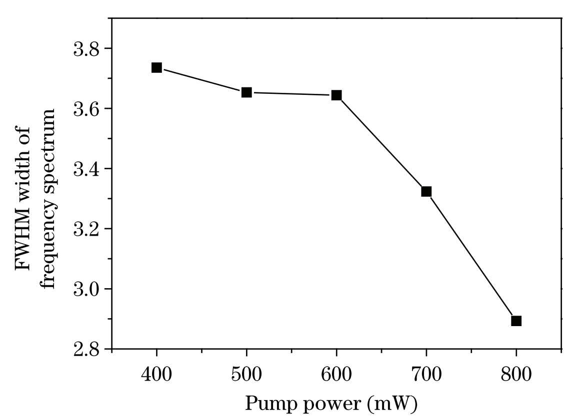

Fig. 3. FWHM of each frequency-domain spectrum under different pump powers.

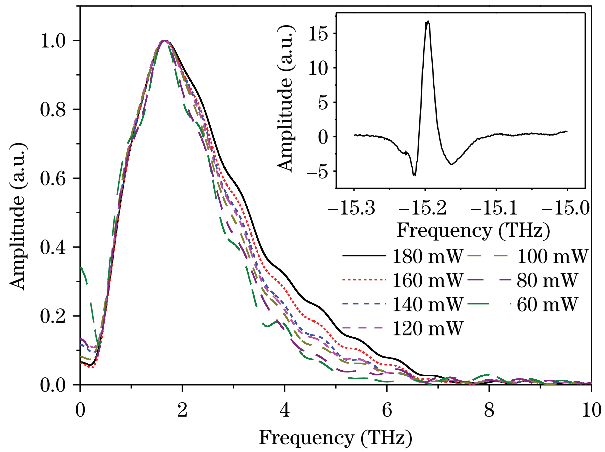

Fig. 4. Normalized amplitude frequency-domain spectrum through fast Fourier transform under different probe powers. Upper right corner: time-domain THz waveform.

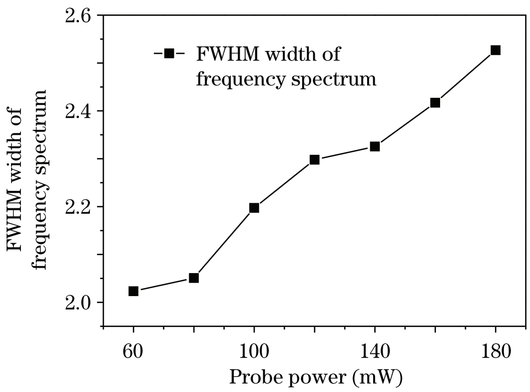

Fig. 5. Bandwidth of each frequency-domain spectrum under different probe powers.

compressed and the degree of self-focusing which can cause the nonlinear effect is also gradually enhanced, adding the amount of pulse compression. Compared with the FWHM of the THz frequency spectrum of 2.02 THz on the 60 mW probe power, it broadens to 2.54 THz because of the pulse compression when the power of the probe increases to 180 mW.

In conclusion, we report the frequency-spectral characterization of THz emission from laser-induced air plasma under different pump and probe powers in ABCD system. As is shown in this letter, when the pump power increases, the collision behavior can cause the bandwidth of the frequency spectrum narrowing. Additionally, since the pulse is compressed as a result of the self-focusing effect, a bandwidth broadening of the THz spectrum is observed with increasing probe power.

This work was supported by the National Natural Science Foundation of China (Nos. 11374007 and 61377109), the Foundation for the Author of National Excellent Doctoral Dissertation of PR China (No. 201237), and the Support Program for Outstanding Ph.D. Advisors (No. YB20101000701).

References

1. H. Hamster, A. Sullivan, S. Gordon, W. White, and R. W. Falcone, Phys. Rev. E **49,** 671 (1994).
2. X. Xie, J. Dai, and X.-C. Zhang, Phys. Rev. Lett. **96,** 075005 (2006).
3. T. I. Oh, Y. S. You, and K. Y. Kim, Opt. Express **20,** 19778 (2012).
4. J. Dai, X. Xie, and X.-C. Zhang, Phys. Rev. Lett. **97,** 103903 (2006).
5. H. Hamster, A. Sullivan, S. Gordon, W. White, and R. W. Falcone, Phys. Rev. Lett. **71,** 2725 (1993).
6. Z.-M. Sheng, K. Mima, J. Zhang, and H. Sanuki, Phys. Rev. Lett. **94,** 095003 (2005).
7. W. Fan, Chin. Opt. Lett. **9,** 110008 (2011).
8. R. Xu, Y. Bai, L. Song, N. Li, P. Peng, and P. Liu, Chin. Opt. Lett. **11,** 123002 (2013).
9. S. Wu, J. Liu, S. Wang, and Y. Zeng, Chin. Opt. Lett. **11,** 101402 (2013).
10. M. Kress, T. Löffler, S. Eden, M. Thomson, and H. Roskos, Opt. Lett. **29,** 1120 (2004).
11. X. Xie, J. Dai, and X.-C. Zhang, Phys. Rev. Lett. **96,** 075005 (2006).
12. I.-C. Ho, X. Guo, and X.-C. Zhang, Opt. Express **18,** 2872 (2010).
13. I.-C. Ho and X-C. Zhang, Appl. Phys. Lett. **98,** 241908 (2011).
14. H.-C. Wu, J. Meyer-ter-Vehn, and Z.-M. Sheng, New. J. Phys. **10,** 043001 (2008).
15. H. Du and N. Yang, Chin. Opt. Lett. **11,** 063202 (2013).
16. H. Harde, R. A. Cheville, and D. Grischkowsky, J. Phys. Chem. A **101,** 3646 (1997).